Tool Wear Estimation Under Different Feed Conditions via Cutting Force Coefficients Derived from Cutting Power Consumption

Jin Ho Park[1,2] – Hae-Sung Yoon[1,2] ✉

[1] School of Aerospace and Mechanical Engineering, Korea Aerospace University, Korea
[2] Department of Smart Air Mobility, Korea Aerospace University, Korea

✉ hsyoon7@kau.ac.kr

Abstract *This study proposes a compact cutting power-based framework for estimating flank wear width (VB) in full-slot end-milling of Ti-6Al-4V under varying feed conditions without additional force sensing systems. Relationships between cutting force coefficients and VB were directly incorporated into an analytical cutting-power model, and the model parameters were identified using ordinary least squares. This formulation yields a closed-form estimator for VB using measured cutting power and process parameters. Milling experiments were conducted at spindle speeds of 800 rpm, 1025 rpm, and 1250 rpm and feed per tooth values of 0.03 mm/tooth, 0.035 mm/tooth, and 0.04 mm/tooth. For each spindle speed, the model was calibrated using the two boundary feed conditions and evaluated at the intermediate condition of 0.035 mm/tooth. The estimated VB generally tracked the measured wear progression, with root mean square error values of 2.88 μm, 14.95 μm, and 14.72 μm at 800 rpm, 1025 rpm, and 1250 rpm, respectively. The proposed approach demonstrates that tool wear can be estimated from cutting power with a limited calibration dataset and provides a simple basis for practical tool condition monitoring within the calibrated feed range.*

Keywords *Ti-6Al-4V, tool wear estimation, cutting power consumption, cutting force coefficients*

Highlights

- *A compact power consumption-based wear model was developed for flank wear estimation under varying feed conditions.*
- *Cutting force coefficient-wear relationships were directly identified using limited calibration data from two boundary feed conditions.*
- *A closed-form estimator enables flank wear estimation using cutting power and process parameters.*

1 INTRODUCTION

Titanium alloys possess excellent mechanical strength, biocompatibility, and corrosion resistance, which have led to their widespread adoption across multiple industries. In aerospace applications, they are commonly used in critical components such as aircraft engine parts and landing gear due to their high specific strength and structural reliability [1,2]. In the biomedical field, their superior biocompatibility enables their widespread use in implantable devices [3,4]. Their corrosion resistance and durability have also promoted their application in energy and power generation systems [5,6]. Across these sectors, the manufactured components must satisfy stringent requirements for dimensional accuracy and surface integrity. Consequently, achieving high machining precision and high-quality surface finishes is essential in the processing of titanium alloys.

To meet the requirements of these sectors, considerable efforts have been devoted to improving the machining accuracy and surface quality of titanium alloys. Li et al. [7] investigated the cutting performance of sinusoidal micro-textured ball-end mills for titanium alloy machining and evaluated the effects on milling force, cutting temperature, and surface roughness. Ju et al. [8] proposed a hybrid machining environment combining cryogenic cooling with nanofluid minimum-quantity lubrication (nMQL), achieving reductions in cutting temperature of up to 25.8 % and residual stress of up to 76.6 %, along with lower tool wear and fewer surface defects. Chi et al. [9] investigated fiber-laser-assisted milling and compared it with conventional milling. The authors observed lower cutting forces and a smoother surface, with surface roughness reduced to approximately 50 % of that of the conventional process.

Meanwhile, cutting tool wear is a critical factor that degrades machining accuracy and surface integrity, thereby affecting final product quality [10]. Tool wear results from multiple interacting mechanisms, including abrasive, adhesive, oxidation/chemical, and diffusion wear [11]. Titanium alloys are widely regarded as difficult-to-cut materials, and their low thermal conductivity limits heat dissipation, promoting heat accumulation at the tool-workpiece interface and accelerating tool wear. Accordingly, extensive research has focused on predicting and monitoring tool wear to determine appropriate tool replacement timing. Pashmforoush et al. [12] proposed a physics-informed machine learning (PIML) framework combining a thermo-mechanical force model with machine-learning regressors to predict flank wear using cutting forces and process parameters. Lee and Yoon [13] introduced a cutting power consumption-based tool life model by integrating cutting power over cutting length, referred to as the accumulated cutting power consumption value (ACPC) to cope with varying cutting conditions and cutting volumes and validated the model under variable feeds and cutting volumes. Liu et al. [14] introduced an in-process monitoring method based on cutting force coefficients and demonstrated their correlation with flank wear.

In practice, cutting conditions in industrial milling are rarely held constant [15]. Feed per tooth, engagement, and material removal rate frequently vary along complex tool paths and across different parts, and this variability can substantially change process signals even at the same wear state. Consequently, wear models calibrated under a

single operating condition may exhibit degraded performance when applied to variable cutting conditions, highlighting the need for approaches that remain effective under practical process variability.

One practical strategy to address this issue is to model wear using cutting force coefficients. While absolute cutting forces are directly affected by changes in chip load and engagement geometry [16], force coefficient-based formulations explicitly incorporate kinematic chip thickness and engagement relationships and decompose the force into shear and edge components [17]. With this structure, the influence of varying cutting conditions can be accounted for within the model, and changes in tool-workpiece interaction effects can be represented by the coefficients. Therefore, coefficient-based representations are generally more suitable for wear modeling across different operating regimes.

However, estimating cutting force coefficients typically requires cutting force measurements using a dynamometer, which requires installing additional hardware and can be costly and intrusive in production environments. In contrast, power consumption signals can be obtained directly from the machine drive system or a power meter without the need for interference in the working volume. For this reason, studies have explored the use of power consumption-based cutting information to estimate cutting force coefficients without additional force sensing systems. Dong et al. [18] formulated coefficient calibration as an optimization problem by linking power consumption to milling force coefficients and demonstrated that force coefficients can be estimated from power signals without force sensors. Shi et al. [19] extracted cutting power by compensating the spindle-speed-dependent idle/drive power from the measured total power and coupled a mechanistic milling force model with a power model; the cutting force coefficients and wear-related parameters were identified via simulated annealing, enabling inverse estimation of flank wear from power measurements. Although these studies demonstrated the feasibility of power-based estimation without direct force measurement, their formulations involved separate coefficient identification or iterative parameter optimization.

For industrial deployment, the tool wear model should be compact and easy to calibrate, since reduced complexity can translate into lower implementation time and cost. Although power-meter-based monitoring has been actively investigated for estimating tool wear without additional sensing systems, many existing approaches still face practical barriers in terms of calibration effort and transferability. Data-driven AI models rely on wear-labeled experimental datasets for training and validation, and reliable prediction requires training data that adequately cover the intended machining conditions [20,21], whereas physics-based models often require substantial effort to characterize thermal/mechanism-dependent conditions and calibrate model parameters from dedicated experiments [22]. Empirical/regression models can be simpler, but they may be formulated with higher-order or nonlinear functional forms and may exhibit limited portability when the operating environment changes [23,24]. Therefore, a low-order model that can be calibrated with a small dataset is highly attractive for shop-floor use, as it enables rapid deployment and efficient recalibration with minimal experimental burden.

This study proposes a compact tool wear estimation model based on cutting power consumption. Cutting power is first obtained by subtracting non-cutting machine system power from the measured total power [25]. Unlike conventional force coefficient-based approaches that rely on cutting force measurements, the proposed method utilizes the relationship between cutting power and cutting force coefficients without requiring direct force measurements. In contrast to the aforementioned power-based approaches involving separate coefficient identification or iterative parameter optimization, the relationships between the cutting force coefficients and flank wear are incorporated directly into the cutting power model. The model parameters are estimated using ordinary least squares (OLS), thereby providing a straightforward calibration procedure without iterative optimization. This formulation yields a closed-form equation for estimating flank wear width (VB) from measured cutting power and process parameters. The model targets full-slot milling at a fixed spindle speed and is designed to operate with limited calibration datasets while enabling interpolative wear estimation within the calibrated feed range. The proposed approach demonstrates the feasibility of practical tool-wear estimation based solely on power measurements, providing a basis for further development toward practical implementation.

2 METHODS AND MATERIALS

This section presents the methodology for modeling tool wear using cutting force coefficients derived from cutting power consumption. The aim is to develop a simple estimator for VB using power consumption signals available from CNC machine tools. The proposed model provides a closed-form linear mapping from cutting power and process parameters to VB, enabling straightforward implementation and calibration.

2.1 Cutting Power Measurement and Separation

In a CNC machine tool, the total power measured by a power meter consists of the baseline power required for machine operation and the additional power consumed during material removal. In the present study, P_{total} was obtained by averaging the measured power over the steady-state machining region, excluding the transient regions associated with tool entry and exit. The non-cutting machine power P_{machine} was obtained from the corresponding air cutting condition without material removal. The cutting power associated with workpiece machining was then calculated as:

$$P_{\text{cutting}} = P_{\text{total}} - P_{\text{machine}} \tag{1}$$

Thus, P_{cutting} represents the average cutting power over the steady-state machining region and serves as the input to the proposed wear estimation model.

2.2 Cutting Power Model Using Cutting Force Coefficients

In end-milling, the instantaneous cutting force is commonly modeled as the sum of a shear component proportional to the undeformed chip thickness and an edge (ploughing) component associated with tool-workpiece contact at the cutting edge (Fig. 1). The differential tangential cutting force is expressed as Eq. (2):

$$dF_t(\theta, z) = \left(K_{te} + K_{tc} f_z \sin\theta\right) dz, \tag{2}$$

where K_{tc} [N/mm²] and K_{te} [N/mm] are the specific and edge force coefficients; f_z [mm/tooth] is the feed per tooth; θ [rad] is the immersion angle of an infinitesimal cutting edge element; z [mm] denotes the axial coordinate along the cutting edge. The term $f_z \sin\theta$ represents the instantaneous undeformed chip thickness, and for full-slot milling the engagement interval is $\theta \in [0, \pi]$.

The differential cutting power can be expressed as the sum of the differential power contributions associated with spindle rotation and feed motion [26]. However, previous studies have reported that, during milling, the mechanical power is predominantly supplied by the spindle-driven cutting action, whereas the feed-drive system contributes relatively little; neglecting the feed term may introduce an approximation error on the order of a few percent or less depending on operating conditions. Xu et al. [27] reported that the spindle motor

power is typically 100 to 1000 times larger than the feed-drive power, allowing the feed contribution to be neglected in cutting power estimation. Li et al. [28] likewise noted that feed power accounts for only a minor portion of the total power under normal cutting conditions and can be omitted in modeling. Consistent with these reports, the feed power for the present machining setup was evaluated at 1025 rpm as $P_{feed}=|F_{feed}|\,V_f/60000$, where $|F_{feed}|$ is the magnitude of the measured cutting force component in the feed direction [N] and V_f is the feed velocity [mm/min]. Relative to the simultaneously measured cutting power, the calculated feed power accounted for only 0.160 % to 0.298 % across the examined feed conditions and cutting lengths. Accordingly, the differential power component associated with feed motion is neglected, and the differential cutting power is approximated as:

$$\mathrm{d}P_{\mathrm{cutting}}(\theta,z)\approx|\mathrm{d}P_n|, \tag{3}$$

where $\mathrm{d}P_{\mathrm{cutting}}$ and $\mathrm{d}P_n$ denote the differential cutting power and the differential power associated with spindle rotation, respectively. Using Eq. (2), $|\mathrm{d}P_n|$ is expressed as:

$$\left|\mathrm{d}P_n(\theta,z)\right|=\left|\mathrm{d}F_t(\theta,z)V_c\right|=\left|\left(K_{te}+f_zK_{tc}\sin\theta\right)\mathrm{d}z\frac{2\pi nr}{60000}\right|, \tag{4}$$

where n [rpm] is the spindle speed; r [mm] is the tool radius. To account for intermittent tooth-workpiece engagement, an engagement function $\Gamma(\theta)$ is introduced:

$$\Gamma(\theta)=\begin{cases}1, \theta_s\le\theta\le\theta_e\\ 0, \text{otherwise}\end{cases}, \tag{5}$$

where θ_s and θ_e [rad] denote the entry and exit immersion angles that define the tooth-workpiece engagement interval, respectively. The average cutting power over one spindle revolution is then expressed as

$$P_{\mathrm{cutting}}=\frac{Z_n}{2\pi}\int_{\theta_1=0}^{\theta_2=2\pi}\int_{z_1=0}^{z_2=a_p}\mathrm{d}P_{\mathrm{cutting}}(\theta,z)\Gamma(\theta)d\theta, \tag{6}$$

where a_p [mm] is the axial depth of cut; Z_n is the number of flutes; θ_1 and θ_2 [rad] are the angular integration limits for the reference cutting edge element over one revolution; z_1 and z_2 [mm] are the axial integration limits along the engaged edge. For full-slot milling, Eq. (6) yields:

$$P_{\mathrm{cutting}}=\frac{nra_pZ_n}{60000}\left(\pi K_{te}+2f_zK_{tc}\right). \tag{7}$$

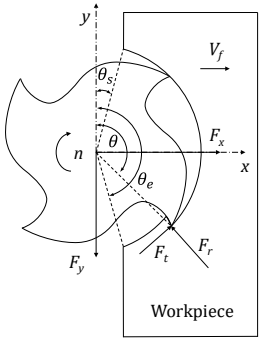


Fig. 1. Schematic diagram of cutting force components in end-milling

2.3 Proposed First-Order Model for Wear Estimation

In general, VB evolves nonlinearly with cumulative cutting length. In the present formulation, the measured VB values are used directly as the wear state variable, while cumulative cutting length is not included as a model variable. Cutting force coefficients have been shown to be sensitive to tool wear and have thus been employed as wear-related quantities for tool condition monitoring [29]. In addition, a linear relationship between edge force coefficients and flank wear area has been experimentally employed for wear estimation [30]. Based on these observations, the relationships between the cutting force coefficients and VB are locally approximated by first-order functions over the wear range investigated in this study. This low-order representation enables a compact formulation and facilitates parameter calibration using limited experimental data. However, as a local approximation, it introduces modeling error that should be considered when interpreting the estimation results. Under this assumption, the cutting force coefficients are expressed as Eqs. (8) and (9):

$$K_{tc}(\mathrm{VB})=\alpha_1VB+\beta_1, \tag{8}$$

$$K_{te}(\mathrm{VB})=\alpha_2VB+\beta_2, \tag{9}$$

where the parameter pairs (α_1,β_1) and (α_2,β_2) correspond to K_{tc} and K_{te}, respectively. Substituting Eqs. (8) and (9) directly into the average cutting power model in Eq. (7) yields

$$P_{\mathrm{cutting}}=C\left[\pi\left(\alpha_2\mathrm{VB}+\beta_2\right)+2f_z(\alpha_1\mathrm{VB}+\beta_1)\right], \tag{10}$$

where

$$C=\frac{nra_pZ_n}{60000}, \tag{11}$$

Equation (10) is linear with respect to the four model parameters α_1, β_1, α_2 and β_2. Therefore, these parameters can be estimated simultaneously using ordinary least squares (OLS). For N calibration observations, Eq. (10) can be expressed in matrix form as:

$$y=X\theta+\varepsilon, \tag{12}$$

where ε is the residual vector, and the parameter vector θ, response vector y, and design matrix X are defined as

$$\theta=\begin{bmatrix}\alpha_1 & \beta_1 & \alpha_2 & \beta_2\end{bmatrix}^T,$$

$$y=\begin{bmatrix}P_{\mathrm{cutting},1}/C\\ P_{\mathrm{cutting},2}/C\\ \vdots\\ P_{\mathrm{cutting},N}/C\end{bmatrix},$$

$$X=\begin{bmatrix}2f_{z,1}\mathrm{VB}_1 & 2f_{z,1} & \pi\mathrm{VB}_1 & \pi\\ 2f_{z,2}\mathrm{VB}_2 & 2f_{z,2} & \pi\mathrm{VB}_2 & \pi\\ \vdots & \vdots & \vdots & \vdots\\ 2f_{z,N}\mathrm{VB}_N & 2f_{z,N} & \pi\mathrm{VB}_N & \pi\end{bmatrix}. \tag{13}$$

The model parameters are estimated by minimizing the sum of squared residuals:

$$\hat{\boldsymbol{\theta}}=\arg\min_{\boldsymbol{\theta}}\left\|\mathbf{y}-\mathbf{X}\boldsymbol{\theta}\right\|_2^2. \tag{14}$$

Because Eq. (14) is a linear least-squares problem, the model parameters can be obtained without iterative optimization. Rearranging Eq. (10) with respect to VB yields the closed-form first-order estimation equation:

$$VB\left(P_{\mathrm{cutting}}\right)=\frac{P_{\mathrm{cutting}}/C-\left(\pi\beta_2+2f_z\beta_1\right)}{\pi\alpha_2+2f_z\alpha_1}. \tag{15}$$

The closed-form estimator in Eq. (15) is intended for use at a fixed spindle speed and full-slot engagement. Once the model parameters are calibrated over a selected f_z range, Eq. (15) can be used to estimate VB from the measured cutting

power and the corresponding f_z value within the calibrated range, provided that n, r, a_p, and Z_n remain unchanged. If spindle speed changes, the model should be recalibrated at the new spindle speed, since the power scaling and the cutting force coefficients may vary with spindle speed.

3 EXPERIMENTAL DETAILS

3.1 Experimental Setup

Figure 2 illustrates the experimental configuration. Milling experiments were carried out on a three-axis CNC machining center (Robodrill α-K10C, FANUC, Japan) using Grade 5 titanium alloy plates (Ti-6Al-4V; Sejin Titanium, Korea). Power consumption was measured with a power meter (PAC4200; Siemens Industry, Germany) and recorded at 0.1 s intervals using LabVIEW. Tool wear was assessed by optical digital microscopy by examining the tool flank face at specified cumulative cutting lengths. Four-flute flat end-mills (Ø12 mm, TSE-4120M-5515, Taegutec Ltd., Daegu, Korea) were employed.

Table 1. The machining parameters

No.	Spindle speed [rpm]	Feed per tooth [mm/tooth]	Axial depth of cut [mm]	Radial depth of cut [mm]
1	800	0.03		
2	800	0.035		
3	800	0.04		
4	1025	0.03		
5	1025	0.035	3	12
6	1025	0.04		
7	1250	0.03		
8	1250	0.035		
9	1250	0.04		

This study reused a subset of the experimental dataset reported in a previous study [23], obtained under identical machining conditions, and performed additional analyses using these data. As shown in Table 1, the machining parameters were spindle speed (n) and feed per tooth (f_z). Each factor was tested at three levels, resulting in nine experimental conditions, and each test was repeated three times. To satisfy the full-slot milling condition assumed in the proposed model, the radial depth of cut (a_e) was fixed at 12 mm (equal to the tool diameter). The axial depth of cut (a_p) was kept constant at 3 mm to isolate the effects of n and f_z.

3.2 Measurement Method of Flank Wear

Flank wear width is defined as the width of the wear land formed on the flank face. As a commonly used tool life indicator, VB was employed in this study, and an end-of-life criterion (300 μm) of VB for uniform flank wear was adopted with reference to the ISO 8688-2 standard [31]. As shown in Fig. 3, VB was measured using an optical microscope and averaged over 10 equally spaced locations along the cutting edge to minimize the influence of spatially non-uniform wear. The first measurement point was located 200 μm away from the tool tip, and subsequent points were taken at 40 μm intervals.

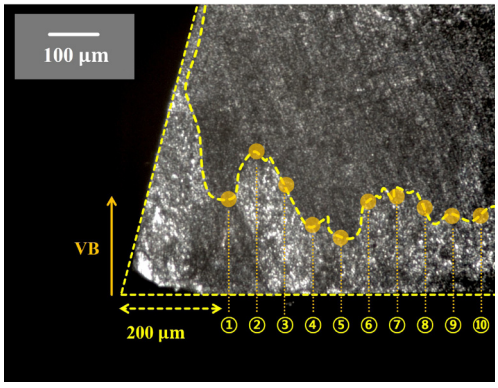


Fig. 3. Flank wear measurement. Reproduced with permission from Ref. [23]

4 RESULTS AND DISCUSSION

4.1 Cutting Power and Model Parameter Identification

Figure 4 presents the variation in cutting power as a function of cumulative cutting length (1000 mm and, thereafter, at 2000 mm intervals from 2000 mm to 8000 mm). For all cutting conditions, the cutting power increased with increasing cumulative length. At a fixed spindle speed, higher f_z produced a higher power level, and in several cases the power difference between f_z levels widened as the cutting length increased. These observations indicate that the required power gradually rises under identical cutting conditions as machining

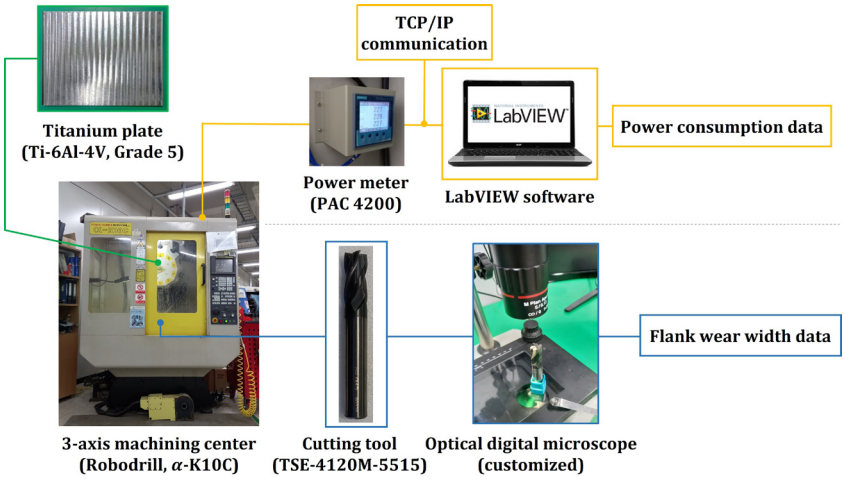


Fig. 2. Experimental setup. Reproduced with permission from [23]

progresses, reflecting changes in tool condition. Therefore, the measured cutting power contains the variations associated with both feed per tooth and tool wear required for calibration of the proposed model.

Figure 5 shows the variation in VB with cumulative cutting length. VB generally increased with increasing cutting length at all spindle speeds. At a given spindle speed, higher f_z generally resulted in larger VB at the same cumulative cutting length, because the increased chip load per tooth promotes faster tool wear [32]. The cutting-power and VB results therefore provide distinct observations of process loading and wear progression under the two boundary feed conditions used for model calibration.

For each spindle speed, the cutting power and VB values obtained from the three repeated experiments were averaged at each feed condition and cumulative cutting length. The standard deviations of the three repetitions were used solely to represent experimental variability in Figs. 4 and 5 and were not treated as additional regression data. The resulting data at f_z of 0.03 mm/tooth and 0.04 mm/tooth over five cumulative cutting lengths provided ten calibration data points. Each cutting power value was paired with the corresponding VB measured at the same feed condition and cumulative cutting length, so that the two boundary feed conditions were retained as separate observations in the regression. The intermediate feed condition, $f_z = 0.035$ mm/tooth, was excluded from parameter identification and reserved for subsequent evaluation.

Using these calibration data, the four model parameters α_1, β_1, α_2 and β_2 were simultaneously identified by OLS according to Eqs. (12)-(14). The identified parameters are summarized in Table 2. The cutting power was then reconstructed using Eq. (10) to quantify the residual fit error of the calibrated first order model. The root mean square error (RMSE) between the measured and reconstructed cutting power was calculated for each spindle speed and is reported as a calibration error rather than an independent validation metric.

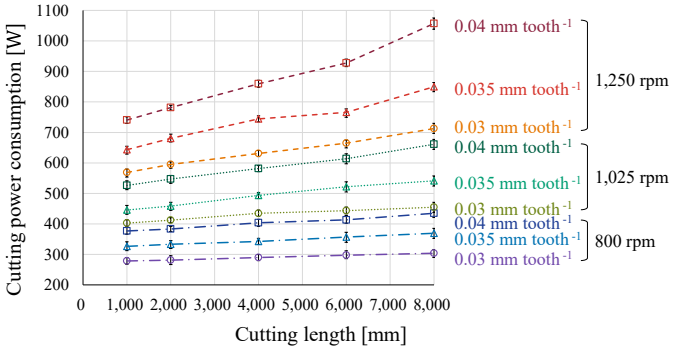


Fig. 4. Cutting power consumption with respect to cutting length

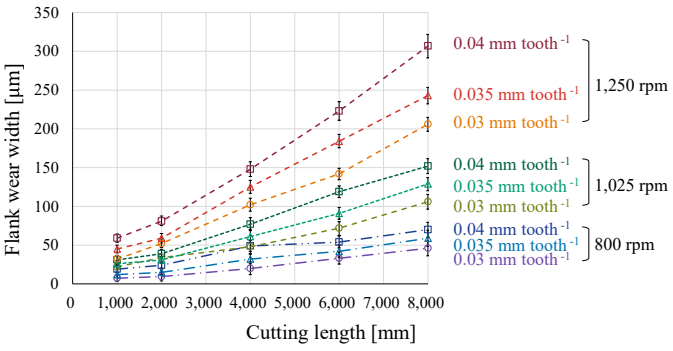


Fig. 5. Flank wear with respect to cutting length

Table 2. OLS-identified model parameters and cutting power calibration RMSE

Spindle speed [rpm]	α_1	β_1	α_2	β_2	Power RMSE [W]
800	27.79	4073.37	−0.24548	12.28	2.39
1025	12.90	4172.73	−0.05976	24.85	5.69
1250	12.67	3936.52	−0.05503	46.38	6.68

4.2 Wear-Dependent Behavior of the Identified Cutting Force Coefficients

The OLS-identified parameters in Table 2 define the wear-dependent relationships of the cutting force coefficients through Eqs. (8) and (9). The identified K_{tc} increased with VB at all spindle speeds, whereas K_{te} decreased with increasing VB. The increase in K_{tc}, which multiplies the chip-load-dependent term in the mechanistic formulation, indicates a progressive rise in the cutting resistance represented by the model.

Figure 6 illustrates the identified first-order relationships at 1250 rpm as a representative example. The markers indicate the K_{tc} and K_{te} values calculated from Eqs. (8) and (9) at the measured VB values corresponding to each feed condition and cumulative cutting length. At the same cumulative cutting length, the two feed conditions exhibit different VB values, and these measured VB values were retained separately in the OLS calibration. As machining progresses, the corresponding positions along the fitted relationships shift toward larger VB, with K_{tc} increasing and K_{te} decreasing.

Within the investigated wear range, K_{te} remained positive at 1025 rpm and 1250 rpm, whereas a slightly negative value occurred only at the highest wear level at 800 rpm. Although K_{te} is conventionally associated with the edge-related friction and ploughing contribution [33], it was indirectly identified here from the cutting power measurements rather than from resolved force components.

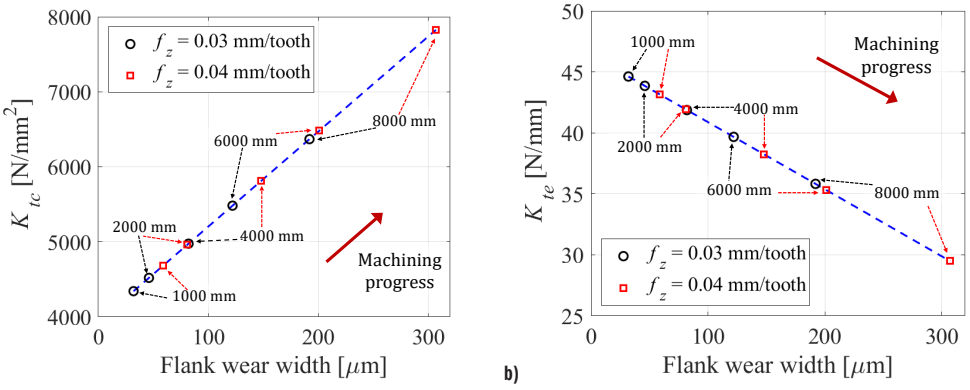


Fig. 6. Representative first-order relationships between flank wear width and cutting force coefficients at 1250 rpm; a) Ktc, and b) Kte

Therefore, the slightly negative value is not interpreted as a physically negative edge force. Even under this condition, the magnitude of $|\pi K_{te}|$ was only approximately 1.7 % to 2.2 % of $|2f_z K_{tc}|$ over the investigated feed range, indicating a minor contribution to the overall power representation.

4.3 Wear Estimation Performance Using Cutting Power

The estimation performance of the calibrated model was evaluated at the intermediate feed condition, f_z = 0.035 mm/tooth, which was excluded from parameter identification. For each spindle speed, the cutting power obtained from each of the three repeated experiments was individually substituted into Eq. (15), together with the corresponding process parameters, yielding three VB estimates at each cumulative cutting length. The mean and standard deviation of the three VB estimates were then calculated to summarize the estimation results. The measured VB values from the three repetitions were likewise summarized by their mean and standard deviation, and the RMSE was calculated between the mean estimated and mean measured VB values over the five cumulative cutting lengths.

Figure 7 compares the measured and estimated VB at 800 rpm, 1025 rpm, and 1250 rpm, with the x-axis representing the measured cutting power corresponding to each cumulative cutting length, as used in Eq. (15) for VB estimation. The estimated values generally tracked the measured progression of wear, with RMSE values of 2.88 µm, 14.95 µm, and 14.72 µm, respectively. The lowest error was obtained at 800 rpm, while comparable errors were observed at 1025 rpm and 1250 rpm. At 1025 rpm, the underestimation was most pronounced at the lowest wear condition, whereas the estimated values more closely followed the measured wear progression at the subsequent wear states. This indicates that the estimation error was larger in the low wear region than at the subsequent wear states.

Based on Eq. (15), the sensitivity of the estimated VB to cutting power is given by $\partial \mathrm{VB}/\partial P_{\mathrm{cutting}} = 1/[C(\pi a_2 + 2f_z a_1)]$. For a fixed spindle speed and feed per tooth, the VB RMSE is related to the cutting power RMSE by the absolute value of this sensitivity. At the intermediate feed condition, the cutting power RMSE values were 3.24 W, 13.15 W, and 15.76 W at 800 rpm, 1025 rpm, and 1250 rpm, respectively, corresponding to the VB RMSE values reported above.

Overall, the results demonstrate that, when calibration is performed separately at each spindle speed using the two boundary feed conditions, the proposed formulation can estimate VB at an intermediate feed condition that was not used for parameter identification. This interpolation capability was observed at all three investigated spindle speeds. Extension of the formulation beyond the calibrated feed range or to different cutting geometries would require additional calibration and evaluation.

From a practical standpoint, the proposed formulation remains compact while avoiding direct cutting force measurement. Compared with force coefficient-based approaches that require direct cutting force measurements and power-based approaches involving more elaborate parameter identification procedures, the proposed method provides a closed-form VB estimator with limited calibration requirements. Once calibrated, the estimator requires only cutting power and the specified process parameters, without additional force sensing systems.

5 CONCLUSION

This study proposed a cutting power consumption-based framework for estimating VB in full-slot end-milling of Ti-6Al-4V without additional force sensing systems. The model parameters were identified directly from cutting power and VB data at two boundary feed conditions using OLS, and the resulting first-order relationships were incorporated into a closed-form VB estimator.

At the evaluated intermediate feed condition, the model yielded RMSE values of 2.88 µm, 14.95 µm, and 14.72 µm at 800 rpm, 1025 rpm, and 1250 rpm, respectively, supporting its interpolation capability within the calibrated feed range. These results show that

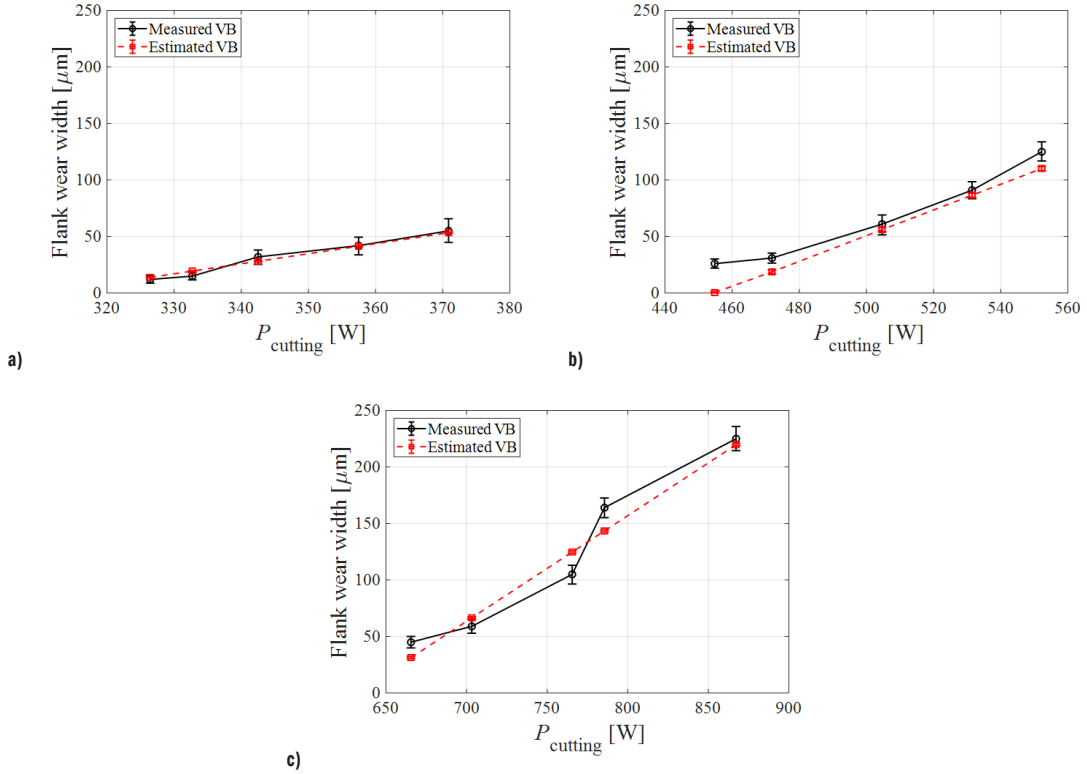


Fig. 7. Comparison of measured and estimated VB with respect to cutting power at the intermediate feed condition (f_z = 0.035 mm/tooth); a) 800 rpm, b) 1025 rpm, and c) 1250 rpm

the proposed formulation can estimate VB at an intermediate feed condition using calibration data acquired at the two boundary feed conditions.

Nevertheless, the limitations associated with the present formulation should be acknowledged. The cutting power model neglects the feed power contribution, and the relationship between VB and the cutting force coefficients is approximated as linear to derive a first-order estimator. These simplifications reduce the implementation and calibration burden but inevitably introduce modeling errors. Therefore, the present model should be interpreted as a practical approximation rather than a fully general representation of wear evolution. In addition, the present evaluation is limited to a fixed cutting geometry and does not establish robustness under variations in cutting geometry or broader machining conditions. Extending the proposed framework to such conditions will require additional calibration data to account for the corresponding changes in cutting power and tool wear behavior. Future work will therefore focus on evaluating and extending the framework under varying cutting geometries and a broader range of operating conditions. Despite these limitations, the main significance of this study lies in demonstrating the feasibility of estimating tool wear from cutting power through a closed-form estimator with limited calibration requirements and straightforward implementation.

References

[1] Boyer, R.R. An overview on the use of titanium in the aerospace industry. *Mater Sci Eng A 213* 103-14 (1996) **DOI:10.1016/0921-5093(96)10233-1**.

[2] Najafizadeh, M., Yazdi, S., Bozorg, M., Ghasempour-Mouziraji, M., Hosseinzadeh, M., Zarrabian, M., Cavaliere, P. Classification and applications of titanium and its alloys: A review. *J Alloys Compd Commun 3* 100019 (2024) **DOI:10.1016/j.jacomc.2024.100019**.

[3] Rack, H.J., Qazi, J.I. Titanium alloys for biomedical applications. *Mater Sci Eng C 26* 1269-1277 (2006) **DOI:10.1016/j.msec.2005.08.032**.

[4] Luo, B., Miu, L., Luo, Y. Titanium alloys for biomedical applications: a review on additive manufacturing process and surface modification technology. *Int J Adv Manuf Technol 137* 3215-3227 (2025) **DOI:10.1007/s00170-025-15287-3**.

[5] Thomas, R. Titanium in the geothermal industry. *Geothermics 32* 679-687 (2003) **DOI:10.1016/j.geothermics.2003.08.004**.

[6] Freitas, B.J.M., Vidilli, A.L., de Bribean Guerra, A., Ferreira, D.C.F., Kasama, A.H., Paes, M.T.P., et al. Ti-6Al-4V and Ti-6Al-4V-0.1 Ru alloys in oil and gas exploration: A review of performance and hydrogen embrittlement. *J Alloys Compd 1019* 179258 (2025) **DOI:10.1016/j.jallcom.2025.179258**.

[7] Li, Q., Wang, B., Ma, C., Guan, Q., Shi, H., Xiao, K., et al. Study on the properties of sinusoidal micro-textured ball end milling cutter for milling titanium alloy. *Stroj Vestn-J Mech Eng 70* 494-506 (2024) **DOI:10.5545/sv-jme.2024.918**.

[8] Ju, S. H., Kim, T.G., Lee, S.W., Choi, H.J., Nam, J. Machinability of Ti-6Al-4V in the milling process using cryogenic cooling and nanofluid MQL. *J Manuf Process 152* 568-578 (2025) **DOI:10.1016/j.jmapro.2025.08.030**.

[9] Chi, Y., Dong, Z., Cui, M., Shan, C., Xiong, Y., Zhang, D., et al. Comparative study on machinability and surface integrity of γ-TiAl alloy in laser assisted milling. *J Mater Res Technol 33* 3743-3755 (2024) **DOI:10.1016/j.jmrt.2024.10.028**.

[10] Akhavan Niaki, F., Mears, L. A comprehensive study on the effects of tool wear on surface roughness, dimensional integrity and residual stress in turning IN718 hard-to-machine alloy. *J Manuf Process 30* 268-280 (2017) **DOI:10.1016/j.jmapro.2017.09.016**.

[11] Sarıkaya, M., Gupta, M.K., Tomaz, I., Pimenov, D.Y., Kuntoğlu, M., Khanna, N. et al. A state-of-the-art review on tool wear and surface integrity characteristics in machining of superalloys. *CIRP J Manuf Sci Technol 35* 624-658 (2021) **DOI:10.1016/j.cirpj.2021.08.005**.

[12] Pashmforoush, F., Ebrahimi Araghizad, A., Budak, E. Physics-informed tool wear prediction in turning process: A thermo-mechanical wear-included force model integrated with machine learning. *J Manuf Syst 77* 266-283 (2024) **DOI:10.1016/j.jmsy.2024.09.008**.

[13] Lee, Y.J., Yoon, H.S. A novel tool life model for varying process conditions and cutting volumes using cutting power consumption. *Int J Adv Manuf Technol 133* 2793-2807 (2024) **DOI:10.1007/s00170-024-13856-6**.

[14] Liu, Y. P., Kilic, Z. M., Altintas, Y. Monitoring of in-process force coefficients and tool wear. *CIRP J Manuf Sci Technol 38* 105-119 (2022) **DOI:10.1016/j.cirpj.2022.04.009**.

[15] Zagórski, I. Surface roughness evaluation of AZ31B magnesium alloy after rough milling using tools with different geometries. *Stroj Vestn-J Mech Eng 70* 355-368 (2024) **DOI:10.5545/sv-jme.2023.885**.

[16] Struzikiewicz, G. Investigation of the titanium alloy turning process with Prime A tools under high-pressure cooling conditions. *Stroj Vestn-J Mech Eng 70* 70-79 (2024) **DOI:10.5545/sv-jme.2023.718**.

[17] Wang, M., Gao, L., Zheng, Y. An examination of the fundamental mechanics of cutting force coefficients. *Int J Mach Tools Manuf 78* 1-7 (2014) **DOI:10.1016/j.ijmachtools.2013.10.008**.

[18] Dong, L., Dang, J., Zhu, Y., Zhang, Y., Wu, B., Mu, C. Prediction method for milling force coefficients based on energy consumption signal in ball-end milling process. *Chin J Aeronaut* 103808 (2026) **DOI:10.1016/j.cja.2025.103808**.

[19] Shi, K., Shi, X., Li, J., Qiang, B., Ren, J., Shi, Y. A novel method for predicting cutting force considering tool wear by power consumption in milling process. *J Manuf Process 149* 632-646 (2025) **DOI:10.1016/j.jmapro.2025.05.065**.

[20] Čuš, F., Župerl, U. Real-time cutting tool condition monitoring in milling. *Stroj Vestn-J Mech Eng 57* 142-150 (2011) **DOI:10.5545/sv-jme.2010.079**.

[21] Truong, T.T., Airao, J., Hojati, F., Ilvig, C.F., Azarhoushang, B., Karras, P., et al. Data-driven prediction of tool wear using Bayesian regularized artificial neural networks. *Measurement 238* 115303 (2024) **DOI:10.1016/j.measurement.2024.115303**.

[22] Wang, C., Ming, W., Chen, M. Milling tool's flank wear prediction by temperature dependent wear mechanism determination when machining Inconel 182 overlays. *Tribol Int 104* 140-156 (2016) **DOI:10.1016/j.triboint.2016.08.036**.

[23] Lee, Y.J., Yoon, H.S. Modeling of cutting tool life with power consumption using Taylor's equation. *J Mech Sci Technol 37* 3077-3085 (2023) **DOI:10.1007/s12206-023-0531-5**.

[24] Bajić, D., Celent, L., Jozić, S. Modeling of the influence of cutting parameters on the surface roughness, tool wear and cutting force in face milling in off-line process control. *Stroj Vestn-J Mech Eng 58* 673-682 (2012) **DOI:10.5545/sv-jme.2012.456**.

[25] Yoon, H.S., Singh, E., Min, S. Empirical power consumption model for rotational axes in machine tools. *J Clean Prod 196* 370-381 (2018) **DOI:10.1016/j.jclepro.2018.06.028**.

[26] Shi, K.N., Ren, J.X., Wang, S.B., Liu, N., Liu, Z.M., Zhang, D.H., Lu, W.F. An improved cutting power-based model for evaluating total energy consumption in general end milling process. *J Clean Prod 231* 1330-1341 (2019) **DOI:10.1016/j.jclepro.2019.05.323**.

[27] Xu, M., Jerard, R.B., Fussell, B.K. Energy based cutting force model calibration for milling. *Comput Aided Des Appl 4* 341-351 (2007) **DOI:10.1080/16864360.2007.10738554**.

[28] Li, L., Yan, J., Xing, Z. Energy requirements evaluation of milling machines based on thermal equilibrium and empirical modelling. *J Clean Prod 52* 113-121 (2013) **DOI:10.1016/j.jclepro.2013.02.039**.

[29] Liu, T., Zhu, K., Wang, G. Micro-milling tool wear monitoring under variable cutting parameters and runout using fast cutting force coefficient identification method. *Int J Adv Manuf Technol 111* 3175-3188 (2020) **DOI:10.1007/s00170-020-06272-z**.

[30] Shahl, A.M., Agarwal, A., Mears, L. Tool wear area estimation through in-process edge force coefficient in trochoidal milling of Inconel 718. *Manuf Lett 35* 391-398 (2023) **DOI:10.1016/j.mfglet.2023.08.072**.

[31] International Organization for Standardization (ISO) Tool life testing in milling Part 2: End milling. ISO 8688-2:1989 from *https://www.iso.org/standard/16092.html*, accessed on 2026-10-28.

[32] Krain, H.R., Sharman, A.R.C., Ridgway, K. Optimisation of tool life and productivity when end milling Inconel 718TM. *J Mater Process Technol 189* 153-161 (2007) **DOI:10.1016/j.jmatprotec.2007.01.017**.

[33] Pan, T., Zhang, J., Zhang, X., Zhao, W., Zhang, H., Lu, B. Milling force coefficients-based tool wear monitoring for variable parameter milling. *Int J Adv Manuf Technol 120* 4565-4580 (2022) **DOI:10.1007/s00170-022-08823-y**.

Acknowledgement *This work was supported by the National Research Foundation of Korea (NRF) grant funded by the Korean government (Ministry of Science and ICT, MSIT) (RS-2026-25473880), the Korea Institute for Advancement of Technology grant funded by the Korean government (Ministry of Trade, Industry and Energy) in 2023 (Project No. P0023691, Specialized Workforce Development Program for Space Materials, Parts, and Equipment),*

and the BK21 FOUR program through the National Research Foundation of Korea (NRF) funded by the Korean government (Grant No. 2120240715457).

Received *2026-04-07,* **revised** *2026-10-06, 2026-10-27,*
accepted *2026-10-28 as Original Scientific Paper.*

Data Availability *The authors confirm that the data supporting the findings of this study are available within the article.*

Author Contribution *Jin Ho Park: Conceptualization, Methodology, Validation, Writing - original draft, Writing - review & editing; Hae-Sung Yoon: Conceptualization, Resources, Funding acquisition, Writing - review & editing, Supervision, Project administration*

Ocena obrabe orodja pri različnih podajalnih pogojih na podlagi koeficientov rezalnih sil, določenih iz porabe moči pri odrezavanju

Povzetek *V raziskavi je predstavljen poenostavljen model za ocenjevanje širine obrabe proste ploskve orodja (VB) pri obdelavi titanove zlitine Ti-6Al-4V s čelnim rezkanjem s polnim radialnim zajemom pri različnih podajalnih pogojih, ki temelji na moči odrezavanja in ne zahteva dodatnih sistemov za merjenje rezalnih sil. Povezave med koeficienti rezalnih sil in širino obrabe VB so bile neposredno vključene v analitični model moči odrezavanja, parametri modela pa so bili določeni z metodo navadnih najmanjših kvadratov. Tako oblikovan model omogoča neposredno oceno širine obrabe VB na podlagi izmerjene moči odrezavanja in procesnih parametrov. Eksperimenti rezkanja so bili izvedeni pri vrtilnih hitrostih vretena 800 min^{-1}, 1025 min^{-1} in 1250 min^{-1} ter podajanjih na zob 0,03 mm/zob, 0,035 mm/zob in 0,04 mm/zob. Za vsako vrtilno hitrost vretena je bil model umerjen na podlagi obeh mejnih vrednosti podajanja, nato pa ovrednoten pri vmesni vrednosti 0,035 mm/zob. Ocenjene vrednosti širine obrabe VB so se na splošno dobro ujemale z izmerjenim potekom obrabe, pri čemer so vrednosti korena srednje kvadratne napake (RMSE) znašale 2,88 µm, 14,95 µm in 14,72 µm pri vrtilnih hitrostih 800 min^{-1}, 1025 min^{-1} oziroma 1250 min^{-1}. Predlagani pristop dokazuje, da je mogoče obrabo orodja ocenjevati na podlagi moči odrezavanja z uporabo omejenega nabora podatkov za umerjanje, ter zagotavlja preprosto osnovo za praktično spremljanje stanja orodja znotraj umerjenega območja podajanja.*

Ključne besede *Ti-6Al-4V, ocenjevanje obrabe orodja, poraba moči pri odrezavanju, koeficienti rezalnih sil*